Infrared Physics and Technology 102 (2019) 103012

Contents lists available at ScienceDirect

Infrared Physics & Technology

journal homepage: www.elsevier.com/locate/infrared

Highly sensitive acetylene detection based on a compact multi-pass gas cell and optimized wavelength modulation technique

Haiyue Sun[a], Yufei Ma[a,*], Ying He[a], Shunda Qiao[a], Xiaotao Yang[b], Frank K. Tittel[c]

[a] National Key Laboratory of Science and Technology on Tunable Laser, Harbin Institute of Technology, Harbin 150001, China
[b] Harbin Engineering University, Harbin 150001, China
[c] Department of Electrical and Computer Engineering, Rice University, 6100 Main Street, Houston, TX 77005, USA

ARTICLE INFO

Keywords:
TDLAS
Trace C_2H_2 detection
Wavelength modulation spectroscopy
Optimum modulation depth

ABSTRACT

A highly sensitive acetylene (C_2H_2) sensor system was demonstrated using tunable diode laser absorption spectroscopy (TDLAS) based on a compact multi-pass gas cell with a 10 m optical path. The sensor system can work in two measurement modes: direct measurements and wavelength modulation (WMS). The incident laser beam with a small spot radius (0.5 mm) effectively eliminated interference fringes and improved the signal-to-noise ratio. The minimum detection limit (MDL) of the direct detection mode was 4.9 ppm. As for the wavelength modulation method, after optimization the modulation depth, a MDL of 14.3 ppb was obtained. The corresponding noise-equivalent absorbance (NEA) was calculated and obtained an excellent value of 1.8×10^{-8} cm^{-1} Hz$^{-1/2}$. An Allan deviation analysis was used to analyze the system stability. The MDL was improved to 1.3 ppb when the averaging time was 270 s.

1. Introduction

Acetylene (C_2H_2) is an important industrial raw material and is widely used in welding, metal cutting and chemical synthesis. However, C_2H_2, with properties of active chemistry and low explosive limit, can threaten people's health and lives as well as the safety of the public property [1,2]. Therefore, it is important to develop a highly sensitive sensor system for trace C_2H_2 detection.

There are various techniques that has been designed for C_2H_2 detection, such as photothermal spectroscopy [3], photoacoustic spectroscopy [4,5] and absorption spectroscopy [6]. Among them, tunable diode laser absorption spectroscopy (TDLAS) has the advantages of the high sensitivity, highly selective and a fast response time [7–9]. Without any manual sample treatment, TDLAS is suitable for online monitoring of the target gas. Based on Beer–Lambert's theory, the detection sensitivity of absorption spectroscopy is proportional to the absorption path [10]. A multi-pass gas cell (MGC) was designed according to Beer–Lambert's law. The long multiple folded path of the MGC is conducive to reduce the volume of the gas sensor system and improve the detection sensitivity [11–13]. Laser sources with single mode play an essential role in the TDLAS technology. A distributed feedback (DFB) laser with a built-in Bragg grating can results in a single mode laser. Due to the excellent monochromaticity and side-mode suppress ratio, the DFB laser is widely in gas detection [14–17]. Compared with other laser sources, it possesses the characteristics of small size, low power consumption and a low cost.

In this paper, a highly sensitive C_2H_2 sensor system based on MGC was demonstrated. Two methods of direct measurements and wavelength modulation spectroscopy (WMS) were studied systematically. The modulation depth of WMS was optimized experimentally. Compared with direct measurements, WMS can reduce the interference of low frequency noise in a gas sensor system [18–21]. The sensor performance for different detect methods including detection limits and linearity were measured and calculated respectively.

2. Analysis of the C_2H_2 sensor system

2.1. Selection of absorption line

Contrary to symmetric diatomic and inert gases, C_2H_2 with a polar structure has various absorption capabilities at different wavelengths. According to the high resolution transmission molecular spectroscopic database (HITRAN), the absorption spectrums of C_2H_2, H_2O and CO_2 from 6520 cm^{-1} to 6550 cm^{-1} were calculated and shown in Fig. 1. We can observe a strong absorption peak at 6534.37 cm^{-1} and the absorption intensity is 1.211×10^{-20} cm^{-1}/(mol × cm^{-2}). The absorption line width was 0.082 cm^{-1}. The absorption intensity of C_2H_2 is much higher (four orders of magnitude) than that of water and CO_2.

* Corresponding author.
E-mail address: mayufei@hit.edu.cn (Y. Ma).

https://doi.org/10.1016/j.infrared.2019.103012
Received 10 May 2019; Received in revised form 8 August 2019; Accepted 8 August 2019
Available online 09 August 2019
1350-4495/

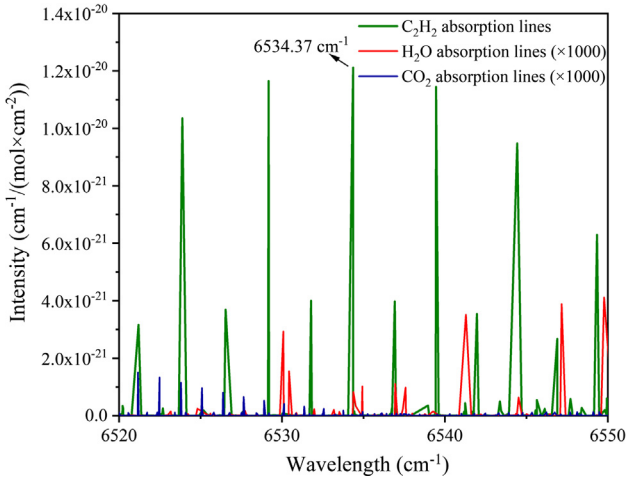

Fig. 1. Absorption lines of C_2H_2, CO_2 and H_2O from 6520 cm^{-1} to 6550 cm^{-1}.

Therefore, CO_2 and water has little influence on the detection of C_2H_2.

A continuous wave (CW) DFB diode laser with a single mode output was used as the laser source to cover this absorption line. The relationship between wavelength, temperature and current of the diode laser was measured and shown in Fig. 2. The selected absorption line (6534.37 cm^{-1}) plotted as a dotted line was in the wavelength tuning range. In order to ensure the suitable wavelength tuning range and working current of the laser source, the operating temperature of 23 °C was selected. When the operating temperature was 23 °C, the wavelength of the output laser can varies from 6535.4 cm^{-1} to 6532.8 cm^{-1} with injected current increasing from 20 mA to 120 mA.

2.2. Theory of direct measurements and WMS technology

Direct measurements of the gas sensors are based on Beer–Lambert's theory. It can be expressed as follows [22,23]:

$$I_t = I_0 \exp[-p \cdot S(T) \cdot \phi(\nu) \cdot C \cdot L] \tag{1}$$

where I_0 is the incident light intensity, I_t is the output light intensity, $S(T)$ is the absorption intensity, $\phi(\nu)$ is the linear function related to temperature, pressure and gas composition, C is the gas concentration, p is the pressure intensity and L is the absorption path. Therefore, the gas concentration C can be calculated from Eq. (2):

$$C = \frac{\int_{-\infty}^{+\infty} -\ln(I_t/I_0)d\nu}{p \cdot S(T) \cdot L} \tag{2}$$

In direct measurements, the gas concentration C can be obtained by reporting the absorbance. The technology without gas calibration is featured by its ease of use. However, energy fluctuations of the laser source and inherent noise of the system are fundamental problems. In consideration of the spectral distribution of sensor system noise, WMS is widely adopted to reduce low-frequency noise and improve signal to noise ratio (SNR). A high frequency sine wave is used to modulate the laser source. The wavelength of the DFB laser can be described as follows:

$$\nu(t) = \bar{\nu} + \delta_\nu \cos(\omega_m t) \tag{3}$$

where $\bar{\nu}$ the wavelength of the scanning signal, δ_ν is the modulation depth, ω_m is the modulation frequency. The absorption coefficient can be described as follows:

$$\alpha(\nu) = CN_0 S\phi(\nu) = \alpha_0 \frac{1}{1 + [(\nu - \nu_0)/\gamma]^2} \tag{4}$$

where N_0 is the total molecular density, ν_0 is the center wavelength of the absorption line. The linear function $\phi(\nu)$ is approximately expressed as the Lorentzian linear function. Spectral line with Gaussian curve can be used at low pressure. Voigt profile with a wide application range was a convolution of a Gaussian with a Lorentzian. In our research, the experiments were carried out at atmospheric pressure. In such condition, the contribution of Gaussian can be neglected and the Voigt line can be properly approximated by a Lorentzian profile [18,24]. γ is the absorption line width. α_0 is the absorption coefficient of the center frequency. In order to simplify this calculation, we identified $\bar{x} = (\bar{\nu} - \nu_0)/\gamma$ and $M = \delta_\nu/\gamma$. $\bar{x}$ and M are the non-dimensional wavenumber deviation from ν_0 and the modulation depth coefficient, respectively. Next, we can substitute the Eq. (3) into the Eq. (4) and expanded the absorption coefficient into a Fourier series:

$$\alpha(\bar{x}) = \alpha_0 [H_0(\bar{x}) + \sum_{n=1}^{\infty} H_n(\bar{x}) \cos(n\omega_m t + n\varphi)] \tag{5}$$

where $n\varphi$ is the delay angle of the WMS technique, $H_0(\bar{x})$ and$H_n(\bar{x})$ are the harmonic coefficients and can be expressed as:

$$H_0(\bar{x}) = \frac{1}{\pi} \int_0^{\pi} \frac{1}{1 + (\bar{x} - M\cos(\theta))^2} d\theta \tag{6}$$

$$H_n(\bar{x}) = \frac{2}{\pi} \int_0^{\pi} \frac{\cos(n\theta)}{1 + (\bar{x} - M\cos(\theta))^2} d\theta \tag{7}$$

At the center frequency ($\bar{x} = 0$), the amplitude of odd harmonic is zero. However, the amplitude of even harmonic reaches the highest values. Because an even harmonic signal decays with the order number and the second harmonic signal is used to retrieve the gas concentration [25,26]. The signal of the sensor system can be expressed as follows:

$$S(\nu) = kT(\nu)P(\nu) = k(1 - \alpha(\nu))P(\nu) \tag{8}$$

$$P(\nu) = P_0(1 + P_\Omega \bar{x} + P_\omega m \cos(\omega_m t)) \tag{9}$$

where k is the conversion constant of the sensor system. $P(\nu)$ was the output power of the laser source. P_0 is the laser power at ν_0. P_Ω and P_ω are the laser power of the scanning signal and modulated signal, respectively. The second harmonics signal of sensor system can be expressed as follows:

$$S(\nu)_{2f} = k\alpha_0 P_0 [(1 + p_\Omega \bar{x}) H_2 \cos(2\omega_m t + 2\varphi)] \tag{10}$$

The theoretical simulation for S_{2f} of the C_2H_2 sensor is showed in Fig. 3. The maximum signal amplitude is obtained when the modulation depth coefficient (M) is 2.2. According to the absorption line width (0.82 cm^{-1}) at 6534.37 cm^{-1}, the optimum modulation depth (δ_ν) was calculated to be 0.18 cm^{-1}.

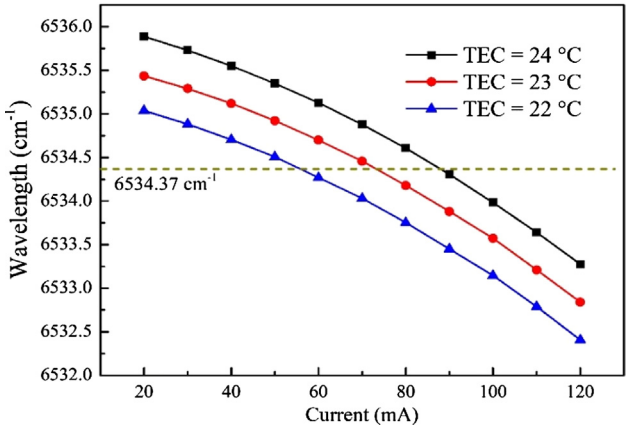

Fig. 2. The relationship between wavelength and current of the diode laser.

3. Experimental setup

The experimental schematic of the C_2H_2 sensor system is shown in Fig. 4. The system is made up of two parts: an electrical unit and an optical unit. In the optical unit, the single mode laser with center

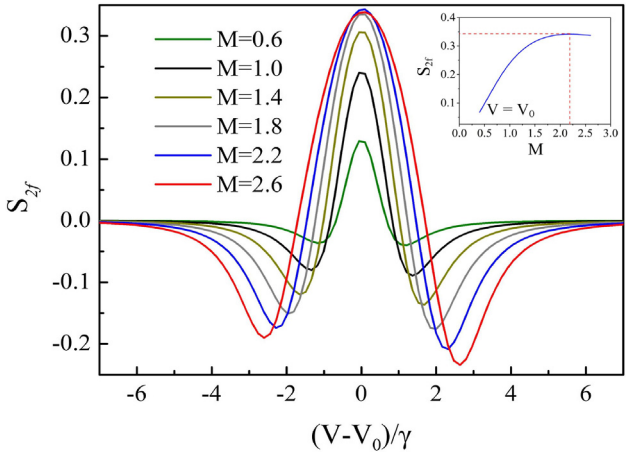

Fig. 3. Second harmonics signal S_{2f} as a function of wavenumber deviation. Insert: S_{2f} as a function of modulation depth coefficient M.

wavelength of 1530 nm was collimated to a parallel light beam. A visible alignment laser assisted in the calibration of the optical system. Two adjustable irises with a minimum aperture of 1 mm were used to control the laser beam spot size and propagation direction of the incident laser. The incident laser with a small spot radius can effectively eliminate interference fringes and improve the signal-to-noise ratio [27,28]. A 34-pass Herriot MGC with an optical length of 10 m is conducive to improve the sensor detection sensitivity. The 34-pass Herriott cell contains two concave mirrors which were coated with gold and protective hafnium oxide (HfO_2) overcoat. The cell volume was 0.24 L, and the window was wedge mirror of calcium fluoride (GaF_2). Two flow controllers with uncertainty of 3% were used to adjust flow rate of C_2H_2 and N_2, respectively, which determined the concentration of C_2H_2 in the cell.

In the electrical unit, the output wavelength of the laser source was controlled by a temperature controller and a current driver. The temperature of the DFB diode laser (Agilecom Fiber Solution Inc., China) was set to 23 °C by TEC. The signal generator 1 produced a low frequency (20 mHz) sawtooth wave used to scan across the C_2H_2 absorption line. Signal generator 2 produced a high frequency (1 kHz) sine wave used as the modulating signal. In the direct measurement, the low frequency sawtooth wave was used as scanning signal and injected into the current driver. An infrared detector converted the output laser from MGC into a voltage signal. In the WMS measurement, low frequency sawtooth and high frequency sine wave were combined by an adder and injected into the laser current driver. The infrared detector converted the output laser into an electrical signal which was sent into the lock-in amplifier. The sine wave also served as a synchronous signal for the lock-in amplifier (Zurich Instruments, Switzerland).

4. Results and discussions

4.1. Direct measurement

C_2H_2 gas with five concentration levels were used as the analyte. The laser current was scanned from 40 mA to 95 mA to cover the absorption line (6534.37 cm^{-1}). The measured points were recorded and shown in Fig. 5. When the laser current was 72.2 mA, there was a strong absorption peak, which corresponds to 6534.37 cm^{-1}. The absorption peak was removed from the spectrum and the remaining data was linearly fitted to obtain a baseline. According to the baseline, the absorbance can be deduced. As shown in Fig. 5(b), the Lorentzian line shape was fitted to retrieve the concentration information. The measured concentration was calculated by the Eq. (2) in Section 2.2. The integral area was depicted in Fig. 6. According to the fitting residual and signal amplitude, the minimum detection limit (MDL) of the C_2H_2 direct sensor system was ~4.9 ppm.

The R squared value for the linear fit was ~0.987. The fitting error and background noise are the main noise sources. WMS technology can solve this problem efficiently and improve the sensor detection sensitivity.

4.2. WMS technique

In the WMS technique, the modulation depth determined the *2f*-WMS signal from the lock-in amplifier. When the concentration of C_2H_2 was 510 ppm, the relationship between the modulation depth and the *2f*-WMS signal was measured and showed shown in Fig. 7(a). The optimum modulation depth of the C_2H_2 sensor system was ~0.182 cm^{-1}. To identify the precision of the sensor system, six different concentrations of C_2H_2 gas severed as analyte. The *2f*-WMS signals with a modulation depth of 0.182 cm^{-1} at different concentrations of C_2H_2 were depicted in Fig. 7(b). As shown in Fig. 8, the linear response of the *2f* signal to C_2H_2 concentration was confirmed by fitting the data with a linear slope. The R square value for the linear fit was 0.999. The noise signal of the sensor system was measured in pure N_2 condition and is also shown in Fig. 8. The standard deviation was 0.0011 μV. The detection limit was calculated to be 14.3 ppb. The noise-equivalent absorbance (NEA) was calculated to be 1.8×10^{-8} cm^{-1} $Hz^{-1/2}$.

The Allan deviation was used to evaluate the stability of the TDLAS sensor system. In the pure N_2 condition, the signal from sensor system was observed for a long period of time. The sampling time was set to 1 s

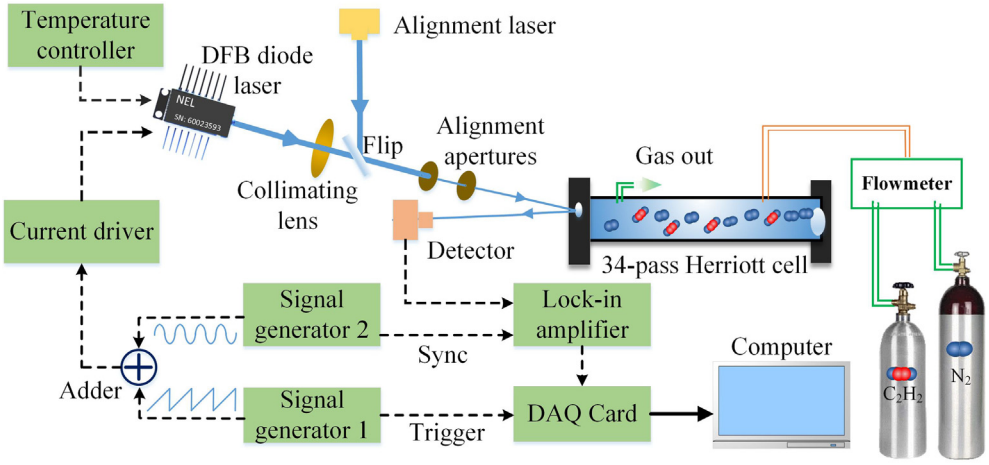

Fig. 4. Experimental schematic of the C_2H_2 sensor system.

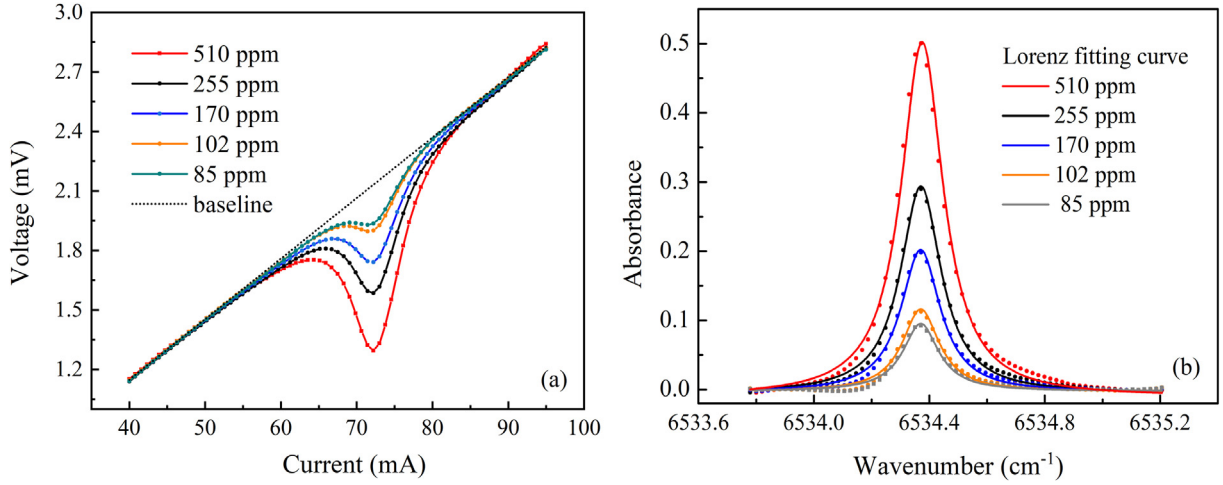

Fig. 5. (a) The absorption of C_2H_2 at 6534.37 cm^{-1}; (b) lorentzian fitting of the absorption line.

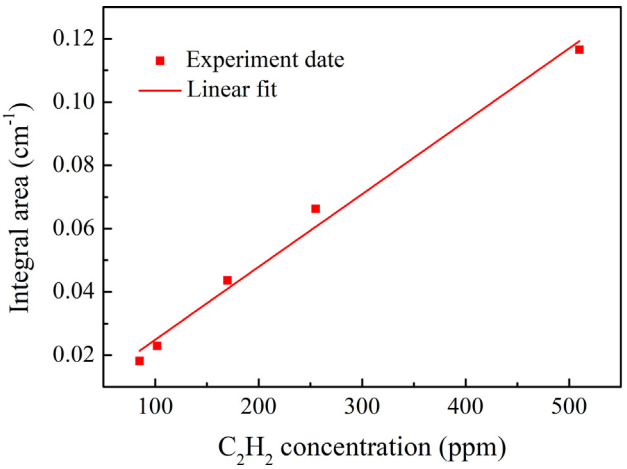

Fig. 6. The integral area at different concentration of C_2H_2.

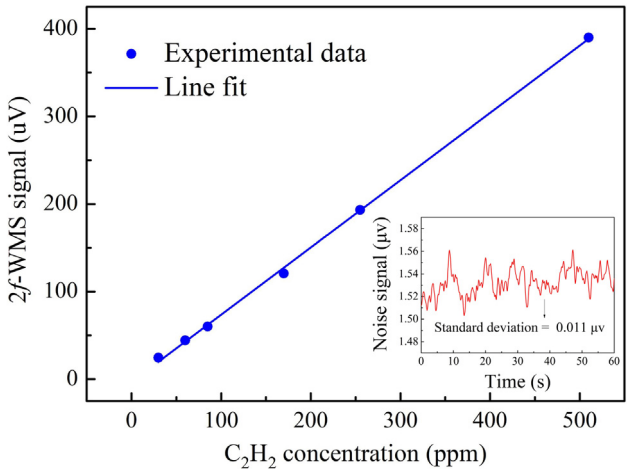

Fig. 8. Linearity and noise of the WMS technology. Insert: noise in a pure N_2 condition.

and 7000 experimental points were obtained during ~2 h. The measured results are shown in Fig. 9. The white noise was the main noise and it was also the random signal in the sensor system. With an increase of the averaging time, the white noise decreased and the MDL was improved to 1.3 ppb when the optimum averaging time was 270 s. The MDL in this research was much better than that of other reported C_2H_2 sensor system (2 ppm in [29] and 0.5 ppm in [30]). But after the optimum averaging time, the system drift noise became dominated and resulted in degradation of the system stability.

5. Conclusions

In this paper, a highly sensitive and stable C_2H_2 sensor system based on a compact MGC with an optical length of 10 m was demonstrated. The small laser beam spot radius (0.5 mm) of the incident laser was

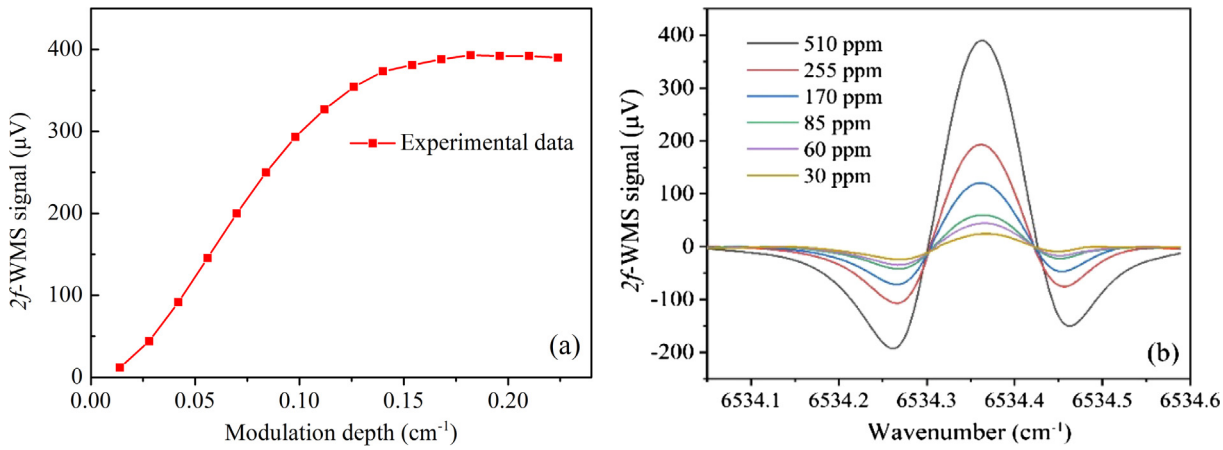

Fig. 7. (a) The *2f* signal amplitude as a function of the modulation depth. (b) The *2f* signal spectrum at modulation of 0.182 cm^{-1}.

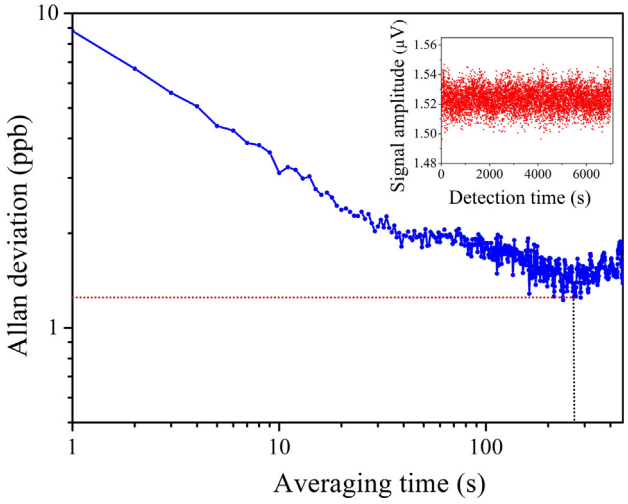

Fig. 9. Allan deviation of pure N_2 gas. Insert: experimental results of N_2 for a 2 h period.

used to eliminated interference fringes and improve the signal-to-noise ratio. In direct measurements, after Lorentzian line shape fitting, the absorbance of the target gases was obtained. The MDL for the direct detection was 4.9 ppm. In the WMS technique, the modulation depth of the C_2H_2 sensor system was optimized to be ~0.182 cm^{-1}. The R square value of the line relationship between the peak value of the 2-*f* signal and the gas concentration was 0.999, which indicated an excellent linear response of C_2H_2 concentration. In the pure N_2 condition, 7000 measurement points were obtained to calculate the Allan deviation of the TDLAS sensor system. A MDL of 1.3 ppb was obtained with an averaging time of 270 s. The corresponding noise-equivalent absorbance (NEA) was calculated and had an excellent value of 7.7×10^{-12} cm^{-1} $Hz^{-1/2}$. The reported C_2H_2 sensor system with high sensitivity and compactness structure has a potential to be used in numerous real-world applications.

Declaration of Competing Interest

The authors declare that they do not have any conflict of interest of this manuscript entitled “Highly sensitive acetylene detection based on a compact multi-pass gas cell and optimized wavelength modulation technique”.

Acknowledgements

This work was supported by the National Natural Science Foundation of China (No. 61875047 and 61505041); Natural Science Foundation of Heilongjiang Province of China (No. YQ2019F006); Fundamental Research Funds for the Central Universities; Financial Grant from the Heilongjiang Province Postdoctoral Foundation (No. LBH-Q18052).

References

[1] Y. Mu, T. Hu, H. Gong, R. Ni, S. Li, A trace C_2H_2 sensor based on an absorption spectrum technique using a mid-infrared interband cascade laser, Micromachines 9 (2018) 530.
[2] Z. Sun, Z. Li, B. Li, Z. Alwahabi, M. Aldén, Quantitative C_2H_2 measurements in sooty flames using mid-infrared polarization spectroscopy, Appl. Phys. B 101 (2010) 423–432.
[3] Y.F. Ma, Y. He, Y. Tong, X. Yu, F.K. Tittel, Quartz-tuning-fork enhanced photothermal spectroscopy for ultra-high sensitive trace gas detection, Opt. Express 26 (2018) 32103–32110.
[4] Y.F. Ma, Y. He, L.G. Zhang, X. Yu, J.B. Zhang, R. Sun, F.K. Tittel, Ultra-high sensitive acetylene detection using quartz-enhanced photoacoustic spectroscopy with a fiber amplified diode laser and a 30.72 kHz quartz tuning fork, Appl. Phys. Lett. 110 (2017) 031107.
[5] Y.F. Ma, Y. He, X. Yu, J.B. Zhang, R. Sun, F.K. Tittel, Compact all-fiber quartz-enhanced photoacoustic spectroscopy sensor with a 30.72 kHz quartz tuning fork and spatially resolved trace gas detection, Appl. Phys. Lett. 108 (2016) 091115.
[6] L. Dong, F.K. Tittel, C.G. Li, N.P. Sanchez, H.P. Wu, C.T. Zheng, Y.J. Yu, A. Sampaolo, R.J. Griffin, Compact TDLAS based sensor design using interband cascade lasers for mid-IR trace gas sensing, Opt. Express 24 (2016) A528.
[7] M. Köhring, S. Huang, M. Jahjah, W. Jiang, W. Ren, U. Willer, C. Caneba, L. Yang, D. Nagrath, W. Schade, F.K. Tittel, QCL based TDLAS sensor for detection of NO towards emission measurements from ovarian cancer cells, Appl. Phys. B 117 (2014) 445–451.
[8] K.Y. Zheng, C.T. Zheng, Q.X. He, D. Yao, L. Hu, Y. Zhang, Y.D. Wang, F.K. Tittel, Near-infrared acetylene sensor system using off-axis integrated-cavity output spectroscopy and two measurement schemes, Opt. Express 26 (2018) 26205–26216.
[9] K. Liu, L. Wang, T. Tan, G.S. Wang, W.J. Zhang, W.D. Chen, X.M. Gao, Highly sensitive detection of methane by near-infrared laser absorption spectroscopy using a compact dense-pattern multipass cell, Sens. Actuat. B 220 (2015) 1000–1005.
[10] D. Herriot, H. Kogelnik, R. Kompfner, Off-axis paths in spherical mirror inter-ferometers, Appl. Opt. 3 (1964) 523–526.
[11] M. Jahjah, W. Ren, P. Stefa'nski, R. Lewicki, J. Zhang, W. Jiang, J. Tarka, F.K. Tittel, A compact QCL based methane and nitrous oxide sensor for environmental and medical applications, Analyst 139 (2014) 2065–2069.
[12] E.R. Crosson, A cavity ring-down analyzer for measuring atmospheric levels of methane, carbon dioxide, and water vapor, Appl. Phys. B 92 (2008) 403–408.
[13] R. Ghorbani, F.M. Schmidt, ICL-based TDLAS sensor for real-time breath gas analysis of carbon monoxide isotopes, Opt. Express 25 (2017) 12743–12752.
[14] C.G. Li, L. Dong, C.T. Zheng, F.K. Tittel, Compact TDLAS based optical sensor for ppb-level ethane detection by use of a 3.34 μm room-temperature CW interband cascade laser, Sens. Actuators B Chem. 232 (2016) 188–194.
[15] A. Sepman, Y. Ögren, M. Gullberg, H. Wiinikka, Development of TDLAS sensor for diagnostics of CO, H_2O and soot concentrations in reactor core of pilot-scale gasifier, Appl. Phys. B 122 (2016) 29.
[16] K. Krzempek, M. Jahjah, R. Lewicki, P. Stefanski, S. So, D. Thomazy, F.K. Tittel, CW DFB RT diode laser based sensor for trace-gas detection of ethane using novel compact multipass gas absorption cell, Appl. Phys. B 112 (2013) 461–465.
[17] Z.H. Du, G. Luo, Y. An, J.Y. Li, Dynamic spectral characteristics measurement of DFB interband cascade laser under injection current tuning, Appl. Phys. Lett. 109 (2016) 011903.
[18] X. Chao, J.B. Jeffries, R.K. Hanson, Absorption sensor for CO in combustion gases using 2.3 μm tunable diode lasers, Meas. Sci. Technol. 20 (2009) 5201–5210.
[19] S. Schilt, L. Thevenaz, P. Robert, Wavelength modulation spectroscopy: combined frequency and intensity laser modulation, Appl. Opt. 42 (2003) 6728–6738.
[20] R.Y. Cui, L. Dong, H.P. Wu, S.Z. Li, L. Zhang, W. Ma, W.B. Yin, L.T. Xiao, S.T. Jia, F.K. Tittel, Highly sensitive and selective co sensor using a 2.33 μm diode laser and wavelength modulation spectroscopy, Opt. Express 26 (2018) 24318.
[21] Q.X. He, C.T. Zheng, H.F. Liu, B. Li, Y.D. Wang, F.K. Tittel, A near-infrared acetylene detection system based on a 1.534 μm tunable diode laser and a miniature gas chamber, Infrared Phys. Technol. 75 (2016) 93–99.
[22] Z.H. Du, J.Y. Li, X.H. Cao, H. Gao, Y.W. Ma, High-sensitive carbon disulfide sensor using wavelength modulation spectroscopy in the mid-infrared fingerprint region, Sens. Actuat. B 247 (2017) 384–391.
[23] B. Li, C.T. Zheng, H.F. Liu, Q.X. He, W.L. Ye, Y. Zhang, J.Q. Pan, Y.D. Wang, Development and measurement of a near-infrared CH_4 detection system using 1.654 μm wavelength-modulated diode laser and open reflective gas sensing probe, Sens. Actuat. B-Chem. 225 (2016) 188–198.
[24] S. Schilt, L. Thevenaz, Wavelength modulation photoacoustic spectroscopy: Theoretical description and experimental results, Infrared Phys. Technol. 48 (2006) 154–162.
[25] Z.R. Zhang, H. Xia, F.Z. Dong, T. Pang, B. Wu, P.S. Sun, G.X. Wang, Y. Wang, Simultaneous detection of multiple gas concentrations with multi-frequency wavelength modulation spectroscopy, EPL-Europhys. Lett. 104 (2013) 44002.
[26] B. Xiong, Z.H. Du, J.Y. Li, Modulation index optimization for optical fringe suppression in wavelength modulation spectroscopy, Rev. Sci. Instrum. 86 (2015) 113104.
[27] C.L. Li, L.G. Shao, H.Y. Meng, J.L. Wei, X.B. Qiu, Q.S. He, W.G. Ma, L.H. Deng, Y.Q. Chen, High-speed multi-pass tunable diode laser absorption spectrometer based on frequency-modulation spectroscopy, Opt. Express 26 (2018) 29330–29339.
[28] C.L. Li, X.Q. Guo, W.H. Ji, J.L. Wei, X.B. Qiu, W.G. Ma, Etalon fringe removal of tunable diode laser multi-pass spectroscopy by wavelet transforms, Opt. Quant. Electron. 50 (2018) 275.
[29] Q. He, H. Liu, B. Li, J. Pan, L. Wang, C. Zheng, Y. Wang, Online detection system on acetylene with tunable diode laser absorption spectroscopy method, Spectrosc. Spectr. Anal. 36 (2016) 3501–3505.
[30] C. Amiot, A. Aalto, P. Ryczkowski, J. Toivonen, G. Genty, Cavity enhanced absorption spectroscopy in the mid-infrared using a supercontinuum source, Appl. Phys. Lett. 111 (2017) 061103.